

Displacement damage study on Tungsten, Iron for fusion neutrons

Mayank Rajput
Institute for Plasma Research, HBNI,
Gandhinagar, India
Email: Mayank.rajput@ipr.res.in

S. Vala
Institute for Plasma Research, HBNI,
Gandhinagar, India

PV Subhash
ITER-India, HBNI
Gandhinagar, India

R. Srinivasan
Institute for Plasma Research, HBNI,
Gandhinagar, India

Abstract

In the present work, study of displacement damage in iron and tungsten has been carried out for fusion neutron irradiation. Prediction of neutron induced displacement per atom (dpa) requires energy spectra data of primary knocked on atoms (PKA) and quantification of Frenkel pair generated due to the produced PKA in the target lattice. In the present work, energy spectra of all the probable PKA species have been calculated with the appropriate nuclear models with TALYS code for all the stable isotopes of tungsten, and iron at upto 15 MeV neutron energy. Number of Frenkel pairs generated from the dynamic of produced PKA in the target atomic lattice of iron and tungsten have been simulated with the molecular dynamics method using the LAMMPS code for PKA of damage energies of upto 200 keV. Time evaluation of vacancies and interstitials have been studied and discussed for iron and tungsten. Results of Molecular dynamics have been compared with the Norgett, Robinson & Torrens (NRT), and athermal recombination-corrected dpa (arc-dpa) methods. Based on the agreement with the MD simulation data, displacement damage cross section of tungsten, and iron have been calculated with the arc-dpa method for neutron irradiation of upto 15 MeV energy. Values of dpa in iron and tungsten have been calculated for neutron spectrum at the first wall of ITER and European demo fusion reactor using the NRT and arc-dpa approach. In tungsten, dpa (arc-dpa) values comes out to be 43 and 16 for 5 year full power operation for European DEMO and ITER machine while for iron, it comes out to be 66 and 25 for 5 year full power operation for European demo and ITER machine respectively.

1. INTRODUCTION

Quantification of displacement damage is an essential parameter to assess the strength and lifetime of functional materials in the ITER and upcoming fusion devices such as European Demo fusion reactor. Fusion neutrons produce different species of primary knocked on atoms (PKA) based on the different reaction channels such as (n,n'), (n,2n), (n, α), (n,p) and (n, γ) etc. Damage cascading of PKA and other knocked on atoms produce vacancies and interstitials, both collectively known as Frenkel pair. Displacement of atoms has adverse effects on the lifetime of reactor materials [1], [2] and quantized with displacement per atom (dpa). Prediction of dpa values is required to accurately predict the lifetime of functional materials to be placed in fusion reactor. dpa is calculated with displacement damage cross section (σ_{dpa}) multiplied with the neutron fluence on any materials. Displacement damage cross section and the values of dpa are calculated as:

$$\sigma_{\text{dpa}}(E_n)_i = \int_{E_d}^{T_{\text{max}}} \left(\frac{d\sigma}{dE}\right)_i v(T)_i dT \quad (1)$$

$$\text{dpa/sec} = \int_0^{E_n} \sigma_{\text{dpa}}(E_n) \cdot \Phi_n dE_n \quad (2)$$

where $\left(\frac{d\sigma}{dE}\right)_i$ is the energy spectra of PKA or recoil atoms from i^{th} reaction channel, $v(T)_i$ is the number of produced Frenkel pair from the dynamics of PKA atom of T energy, E_n is the energy of incident neutron, E_d is the displacement threshold energy of target lattice, T_{max} is the maximum energy available for displacement damage and Φ_n is the neutron flux on the material. Energy spectra of PKA from each open reaction channel can be calculated with the nuclear codes such as TALYS-1.8 [3] and Empire-3.2 [4]. Mayank et al [5,6,7] have studied the energy differential cross section (EDX) of outgoing particles from neutron induced reactions on chromium, tungsten, & iron. Dynamics of PKA creates Frenkel pairs that can be calculated with Norgett, Robinson and Torrens (NRT) method [8], Athermal recombination- dpa (arc-dpa) method [9] and Molecular dynamics method [10]. NRT method is the basic method of damage evaluation that is used in the materials optimization for ITER

and upcoming fusion reactors [9]. Molecular dynamics simulation [10] includes the annihilation and recombination of vacancies and interstitials in its approach and can also provide insight into the time evaluation of defects, thus considered as one of the most accurate method to predict the number of displacements. Athermal recombination corrected dpa (arc-dpa) method is the modification in the NRT approach that additionally include the defect generation efficiency [9]. Arc-dpa method [9] predicts values of displacement damage close to the MD simulations. Previously, Molecular dynamics study of damage evaluation in tungsten have been carried out by Warriar et al [11], and Fikar et al [12] at up to 50 keV damage energy of PKA. For studying the radiation damage by PKA, Stoller et al [13, 14] had carried out the MD simulation for iron at up to 50 keV damage energies of PKA. In the present work, Molecular dynamics simulations have been carried out at up to 200 keV damage energies of PKA in tungsten, and iron in the [1,0,0], [0,1,0] and [0,0,1] directions. Number of defects calculated with MD simulations have been compared with the results of NRT, and arc-dpa methods. MD simulations have been carried out with the Large-scale Atomic/Molecular Massively Parallel Simulator (LAMMPS) code [15]. Based on the comparison of MD simulation results, displacement cross section of tungsten, and iron have been calculated with arc-dpa method. Values of dpa in tungsten and iron have been calculated for first wall neutron spectrum of ITER and European demo reactor.

2. METHODOLOGY AND CALCULATIONS METHODS

2.1 Differential cross section of pka

To calculate the energy spectra of PKA, TALYS 1.8 [3] and Empire 3.2 [4] codes have been used. Different nuclear models are selected in TALYS-1.8 code to get the best fitted calculated data with the existing experimental data for the iron. Comparison of calculated data with the existing experimental data, and nuclear data from ENDF and TENDL data libraries have been discussed in the results and discussion section. For (n,p) and (n,np) reaction channels in iron, compound nuclear reaction mechanism is calculated with Hauser Feshbach model with Moldauer width fluctuation factor, pre-equilibrium reaction calculations is calculated with the multistep compound nuclear model and back shifted fermi gas model is used for level density parameters. And for (n, α), (n,2n), (n,Y) and (n,n') reaction channels in iron, pure Hauser Feshbach model is adopted for compound nuclear calculations, pre-equilibrium calculations have been carried out using the multi-step compound model and constant temperature and Fermi gas model has been adopted for level density parameters. For tungsten, Nuclear models and parameters have been adopted from Mayank et al [6].

2.2 Molecular dynamics study of displacement cascades

Molecular dynamics simulations are the computational approach to model the atomic systems for simulating the displacement cascades. Position of all the atoms in the solid lattice is monitored at different stages of cascade development. In the present work, Molecular dynamics simulations have been carried out with the LAMMPS code [15]. LAMMPS code solves the Newton's equation of motion numerically over the time span of up to few nanoseconds using the interatomic potentials of interactions between PKAs and solid lattice. MD simulation has limitations of sample size (up to the solid of micron size) and time span (upto 10 ns) that it can simulate. It includes many body effects and provides the insight into the spatial distribution of interstitials and vacancies as well as the time evaluation of displacement damages. In the present work, cascade simulations are initiated by giving an atom a specified energy and initial direction, and later location of each atom is monitored at the time interval of 0.1picosecond. Location of each atom is later used in the quantification and visualisation of interstitials and vacancies using the Ovito tool [16]. In the Ovito tool, Wigner-Seitz analysis has been performed to simulate the time evaluation of interstitials and vacancies. In Wigner-Seitz analysis, locations of atoms have been checked in each Wigner-Seitz cell. In the present work, cascading of radiation damage has been simulated for damage energy of 5 keV, 30 keV, 50 keV, 100 keV and 200 keV for native PKA species in tungsten and iron. For tungsten, interatomic potentials are based on the work of Zhou et al [17] and previously used by Warriar et al [11] in simulation of PKA cascading in tungsten at up to 5 keV energy have been used in this work. For iron, interatomic potential have been taken from Malerba et al [18]. PKA of above-mentioned energies have been generated in [1,0,0], [0,1,0] and [0,0,1] directions. Periodic boundary conditions have been used in these simulations so that no interstitial and vacancy would be lost or stopped at the boundaries of target lattice. Sample size of target lattice, and number of atoms in the lattice have been given in table I. Number of Frenkel pair after the generation of PKA have been calculated at each 0.1 picosecond to up to 20 picoseconds. Results from MD simulations and Wigner-Seitz analysis have been explained in the results and discussion section (Sec. 3.2).

Table I details of parameters considered in the MD simulation of PKA cascades

Sample	Damage energy of PKA (keV)	Sample size (Angstrom)	Number of atoms in sample
Tungsten (BCC) (Lattice constant= 3.16)	5	189*189*189	15,60,000
	30	316*316*316	28,74,686
	50	379*379*379	42,89,420
	100	442*442*442	66,84,280
Iron (BCC) (Lattice constant = 2.87)	5	172.2*172.2*172.2	15,60,000
	30	287*287*287	28,74,686
	50	344*344*344	42,89,420
	100	401*401*401	66,84,280
	200	487*487*487	100,82,748

2.3 NRT and Arc-dpa method

Primary knocked on atoms lose their energy in any solid via collision with electrons and via collision with atoms. Energy loss of PKA with electrons contribute to electronic excitation and collision with atoms contribute to the displacement damage. Norgett, Robinson and Torrens (NRT) [8] proposed a method to predict the displacement in solid based on the damage energy where damage energy is energy of PKA minus the energy loss in electronic losses. As NRT model does not include recombination and relocation of atoms in its approach, Arc-dpa approach to predict the displacement damage have been proposed by Nordlund et al [9] by modifying the NRT formulation as:

$$\nu(T) = \frac{0.8}{2Ed} \cdot T_{\text{dam}} \cdot \epsilon_{\text{arc-dpa}} \quad (3)$$

$$\epsilon_{\text{arc-dpa}} = \frac{1 - C_{\text{arc-dpa}}}{(2Ed/0.8)^{b_{\text{arc-dpa}}}} T_{\text{Dam}}^{b_{\text{arc-dpa}}} + C_{\text{arc-dpa}} \quad (4)$$

Where $\nu(T)$ is the number of Frenkel pair, $\epsilon_{\text{arc-dpa}}$ is the defect generation efficiency, and $C_{\text{arc-dpa}}$, $b_{\text{arc-dpa}}$ are the constants of arc-dpa method. Constants $C_{\text{arc-dpa}}$, $b_{\text{arc-dpa}}$ are either calculated with the fitting of the experimental data or fitting with the data from molecular dynamic simulations. In the present work, these constant parameters have been taken from Nordlund et al [9] for tungsten. And for iron, constant parameters were fitted with the MD simulation results of present work. T_{dam} is the damage energy available to the PKA for the cascade damage and calculated with the formulas of NRT approach [8]. Details of constant parameters for arc-dpa and their values have been given in the section 3.3.

3. Results and discussion

3.1 Selection of nuclear models

To select the appropriate nuclear models and parameters, EDX data of outgoing particles (neutrons, protons and alpha particles) have been calculated and compared with the experimental data from EXFOR and nuclear data from ENDF-VIII [19] and TENDL-15 [20]. In the energy spectra of outgoing neutrons, neutrons from (n,el), (n,inel), (n,np) and (n,2n) reaction channels have been included. EDX of outgoing particles are calculated with the TALYS-1.8 code (with selected nuclear models) and EMPIRE-3.2 (default nuclear models). Calculated EDX from TALYS code have been compared with data from Empire calculations (default nuclear models), experimental data from Kozyr et al [21], Grimes et al [22], Fischer et al [23], and evaluated data from TENDL-2015, and ENDF/B-VIII data libraries. This comparison has been presented in the fig. 1 for neutrons and protons. It is noted from the calculations of EDX for outgoing neutrons that calculated EDX of neutrons with TALYS code are in good agreement with the experimental data at up to 10 MeV. At higher energies outgoing neutrons (10-14 MeV), calculated data is not in agreement with the experimental data which is due to contribution of neutrons from discrete inelastic scattering and elastic scattering in the calculated data in this energy range which was not accounted in the experimental data of Kozyr et al. Kozyr et al [21] had reported only inelastic scattering cross sections at 14.1 MeV incident energy neutrons. EDX data from Empire code, underestimates the experimental data at low outgoing neutron energies of 0-2 MeV energy region. The deficiency of TENDL-15 data, shown in fig. 1 is a result of inappropriate calculation of the total energy spectrum of outgoing neutron in the data library. EDX data from the TENDL-2015 and ENDF/B-VIII are not in the good agreement with the experimental data for outgoing particles. TENDL data library is written with the TALYS code using the default and modified nuclear models and parameters and ENDF/B-VIII data library has been evaluated with the Empire code with its default and modified nuclear models. It overestimates the experimental data in the 0-4 MeV energy range of outgoing neutrons. Experimental data of EDX of outgoing protons and alpha particles from Grimes et al [22] and Fischer et al [23] are also compared with the calculated EDX data from TALYS code and found to be in good agreement

for both the ejectiles. It is concluding after the calculation of EDX of outgoing particles that EDX calculated with the selected nuclear models are in better agreement than the ENDFVIII and TENDL-15.

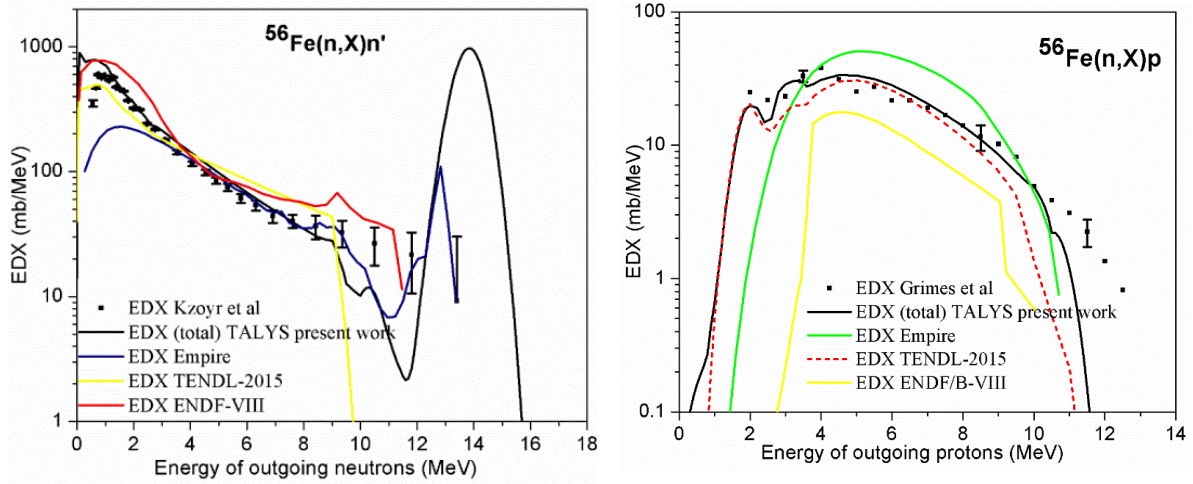


Fig. 1 EDX of outgoing neutrons and protons from neutron induced reactions on ^{56}Fe at 14.1 MeV energy

3.2 Calculation of energy spectra of PKA

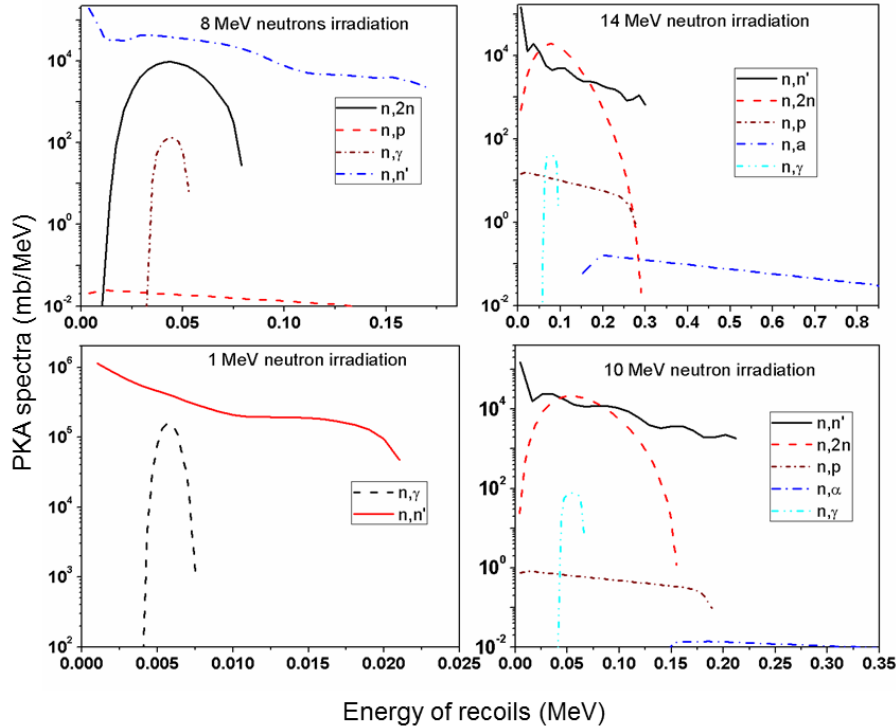


Fig. 2 energy spectra of PKA from ^{184}W at incident neutron energies of 1, 8, 10, 14 MeV

Energy spectra of PKA from ^{184}W have been calculated for neutrons of 1, 6, 10, 14 MeV energy and presented in the fig. 2. It is noted from the energy spectra of PKA from ^{184}W that contribution from (n,2n), (n,p) are open for high energy neutrons as threshold energy for these reaction channels are 7.451 MeV, 2.095 MeV while other reaction channels such as (n,n'), (n, α), and (n, γ) are open even for thermal neutron energies. But (n, α) reaction channel has very low reaction cross section for incident neutrons of up to 10 MeV energy. Similar to this, energy spectra of PKA have also been calculated for other stable isotopes of tungsten (^{180}W , ^{182}W , ^{183}W , ^{184}W & ^{186}W) and iron (^{54}Fe , ^{56}Fe , ^{57}Fe , & ^{58}Fe). PKA spectra are later used in the eq. 1 to calculate the displacement damage cross section of tungsten and iron.

3.3 Damage cascade and calculation of Frenkel pair

It is noted in the calculation of energy spectra of PKA that PKA of upto 500 KeV energies are produced from tungsten and iron at fusion neutron energies [6,7]. In the present work, PKA cascading has been simulated upto

200 keV damage energy and its effects on the displacements of atoms have been recorded at the time interval of 0.1 Pico second. PKA of 5 keV, 30 keV, 50 keV, 100 keV and 200 keV damage energies are generated in the sample and displacements in atoms have been recorded as a function of time for iron and tungsten. Damage cascade in tungsten at 5 keV damage energy is presented in fig. 5 for different time stages of damage cascading. In the fig. 3, it is noted that at the beginning of the cascade, vacancies and interstitials are less in number (at 0.6 pico second). But as the time increases, numbers of defects increases and reaches to the maximum value at 1 pico second. This maximum number of Frenkel pair represent the collisional stage of damage cascade. After this vacancies and interstitials tend to recombine with the each other and their number decreases as they occupy the interstitial and vacant sites in the lattice (near to 2 pico second for 5 keV PKA damage energy). Beyond that time, defects tends to stabilize and their number further decreases to the minimum saturated value (near to 6 pico second). This stage represents quenching stage of displacement cascade.

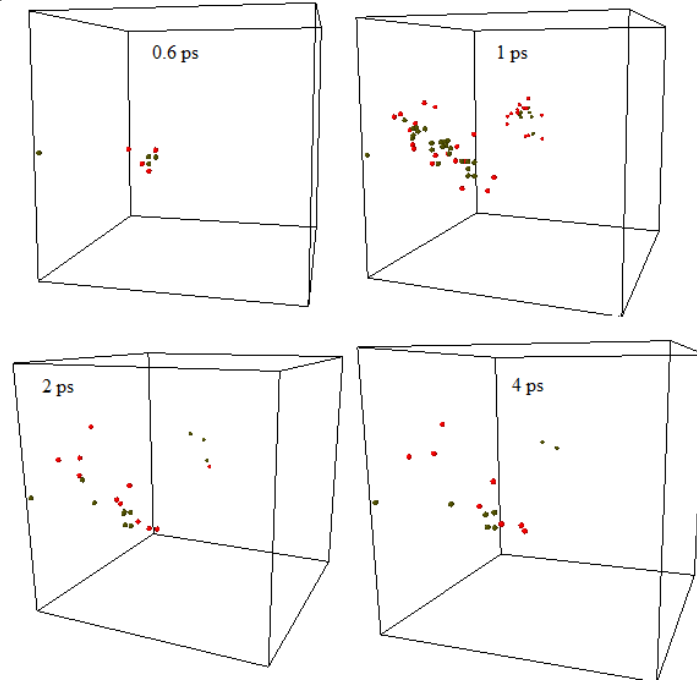


Fig. 3 Visualisation of vacancies (red) and interstitials (black) in the tungsten cascade for 5 keV PKA at different time from PKA formation

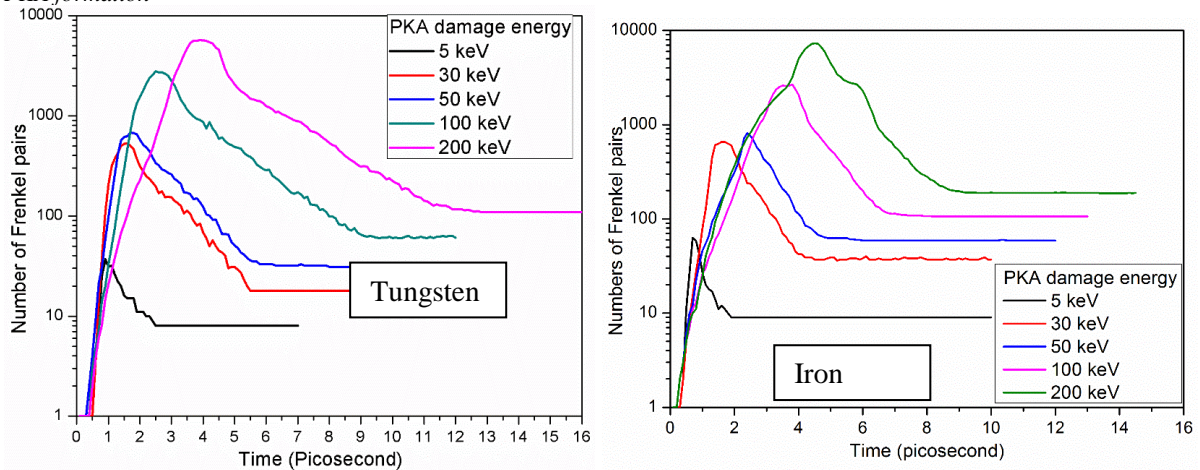


Fig. 4 Number of Frenkel pairs vs time for different PKA energies in tungsten and iron

Number of Frenkel pairs have been calculated at the time interval of 0.1 pico second for PKA of damage energies of up to 200 keV. Number of Frenkel pair vs time for tungsten solid and iron solid lattice has been plotted in fig. 4 to understand the dynamics of defects at different energies. It is noted from the fig. 4 that number of defects reaches to its peak value and then knocked on atoms tend to attain the vacant and interstitials position in the lattice thus decreasing their number to form stable defects.

3.4 Comparison of MD simulation, NRT and arc-dpa method

In the present work, Number of Frenkel pair have been calculated with the arc-dpa and NRT method for native PKA species in iron and tungsten. Results of NRT, arc-dpa methods have been compared with the result of MD simulations. Based on the comparison between arc-dpa method and MD simulation of native PKA species in iron and tungsten, constant parameter of arc-dpa method have been selected and later used to calculate the damage matrices or the numbers of Frenkel pair from other PKA species in iron and tungsten. At lower energies (<100 eV), NRT, arc-dpa and MD simulations predict similar number of Frenkel pair. As the energy of PKA increases, NRT model start deviating from MD simulations and predicts values higher than MD simulations. Constant parameters for arc-dpa method have been given in the table II.

Table II constant parameter for arc-dpa method

Parameter	Values		Reference
	$b_{\text{arc-dpa}}$	$c_{\text{arc-dpa}}$	
Iron	-0.586 ± 0.01 -0.71 ± 0.01	0.31 ± 0.09 0.12 ± 0.02	10 Based on present MD simulations
Tungsten	-0.56 ± 0.02	0.12 ± 0.01	10

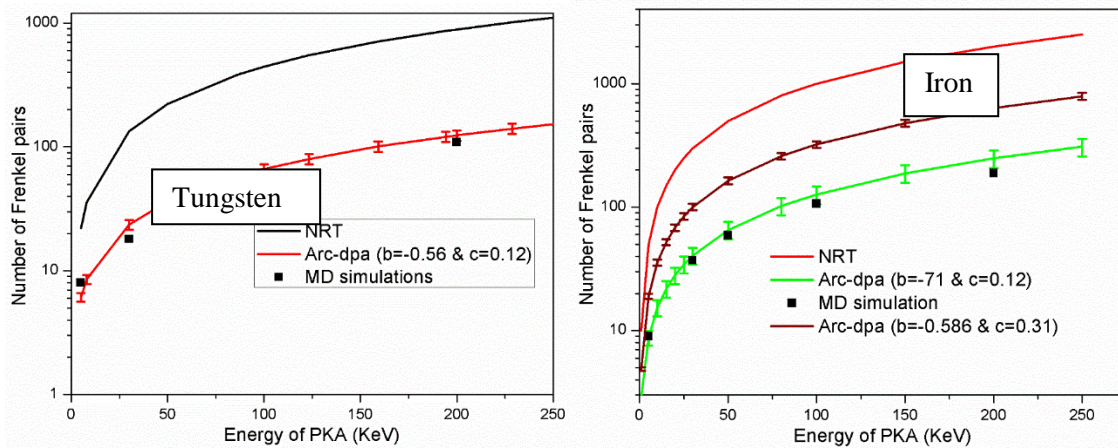


Fig. 5 number of Frenkel pair calculated with MD simulation, NRT and arc-dpa approach for Fe PKA in Fe target lattice and W PKA in W lattice

Based on the constant parameters, given in table II, number of Frenkel pairs, generated due to energetic knocked on atoms have been calculated with NRT, and Arc-dpa method. Arc-dpa method for tungsten compares well with the MD simulations using the given constant parameters [9]. For iron, Frenkel pair calculated with arc-dpa method using the constant parameters from Nordlund et al [9] overestimates the MD simulation data. Nordlund et al [9] have calculated the $b_{\text{arc-dpa}}$ and $c_{\text{arc-dpa}}$ based on the MD simulation data of Stoller et al. Stoller et al had simulated the native iron PKA in the iron lattice using the MOLDY code [24] and had used the effective sphere identification method for analysing the displacements in the lattice and data were not corrected for interstitials and vacancy structures [14] thus overestimate the number of Frenkel pair in their calculations. For iron, constant parameters have been fitted with the present results of molecular dynamics. Frenkel pair calculated with fitted parameters are in good agreement with the MD simulations (fig 5). These constants parameters of iron and tungsten have been used to quantify the displacement damage due to other PKA species from other open reaction channels in the iron and tungsten.

3.5 Displacement damage cross section of tungsten and iron

All the open reaction channels have been considered in the calculation of displacement damage cross section with the NRT and arc-dpa method and presented in the fig. 6 for the natural iron and tungsten for incident neutrons of up to 15 MeV energy. Increase in the displacement cross sections beyond 11 MeV energy is due to significant contributions from (n,np) and (n,2n) reaction channels. Displacement cross section of iron comes out to be more than the displacement cross section of tungsten due to high reaction cross section and low threshold for damage production compared to tungsten.

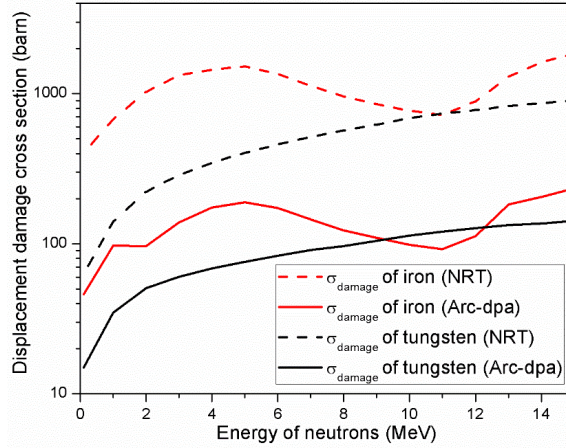


Fig. 6 displacement damage cross section of natural iron and tungsten with arc-dpa methods for neutron irradiation of up to 15 MeV energy

3.6 dpa values in tungsten and iron for ITER like environment using neutron fluence

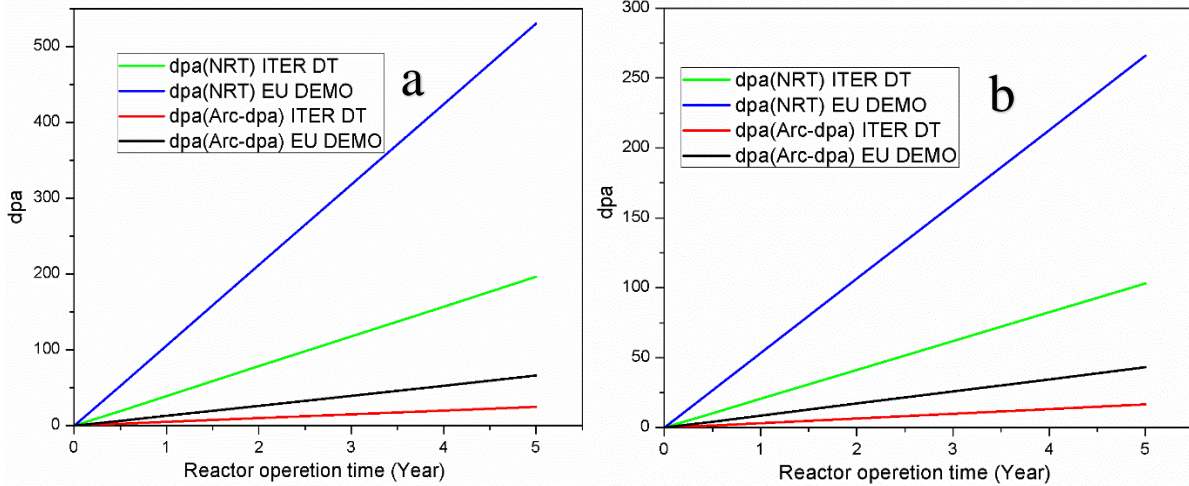


Fig. 7 Values of dpa in the iron (fig. 11. a) and dpa in tungsten (fig. 11. b) for the neutron spectrum at first wall material from ITER DT campaign and EU DEMO fusion reactor

Displacements per atom which is key parameter in defining the lifetime of functional materials in fusion reactors have been calculated for first wall neutron spectrum of ITER (DT campaign) and European DEMO reactor [25]. Neutron spectrum of ITER first wall and European DEMO first wall have been taken from Gilbert et al [25]. Dpa values in the iron and tungsten have been calculated with the NRT and Arc-dpa approach as the function of time and have been presented in fig. 7. In iron, 66 dpa (arc-dpa) is observed for five-year reactor operations in the EU demo reactor approach while 25 dpa will be formed in 5-year operation of ITER DT campaign. Similarly, for Tungsten, 43 dpa is observed in the tungsten for EU Demo and 16 dpa for ITER DT campaign. Tungsten preferentially comes out to be more radiation resistant due to high threshold energy for displacement damage and low activation material compared to iron.

4. Summery and conclusion

Energy spectra of PKA from neutron induced reactions and quantification of Frenkel pair by the energetic PKA are the two essential input parameters that are required to evaluate the dpa in fusion reactor materials. In the present work, energy spectra of PKA from all the open reaction channels from all the stable isotopes of tungsten (^{180}W , ^{182}W , ^{183}W , ^{184}W , & ^{186}W) and iron (^{54}Fe , ^{56}Fe , ^{57}Fe , & ^{58}Fe) have been predicted with the appropriate nuclear models with the TALYS code. Quantification of Frenkel pair produced by the energetic native PKA in iron and tungsten for the damage energy of 5, 30, 50, 100 & 200 keV have been carried out with MD simulation using the LAMMPS code. Results of MD simulations have been compared with the results of NRT and arc-dpa method. Frenkel pairs predicted with arc-dpa method using the constant parameters from Nordlund et al are in good agreement with MD simulation results for tungsten and overestimate the results of MD simulation for iron. For iron, constant parameters ($b_{\text{arc-dpa}} = -0.71 \pm 0.001$, $b_{\text{arc-dpa}} = -0.12 \pm 0.002$) have been fitted with the present MD simulation results. Based on the results of energy spectra and damage matrices from arc-dpa method and NRT

approach, displacement damage cross section have been calculated for iron and tungsten. dpa values in iron and tungsten have been calculated for neutron spectrum of first wall in ITER machine and European Demo fusion reactor. dpa value in iron with the arc-dpa approach reaches upto 25 and 66 for ITER and European demo for five-year reactor operation while in tungsten, it reaches upto 16 and 43 for ITER and European Demo reactor for five-year reactor operations. Similar assessment of dpa can also be carried out for other important fusion reactor materials.

5. References:

1. V. Barabash et al. Materials challenges for ITER – Current status and future activities *Journal of Nuclear Materials* 367-370 (2007) 21–32.
2. G. Federici *et al* 2017 European DEMO design strategy and consequences for materials *Nucl. Fusion* **57** 092002.
3. A. J. Koning et al Modern Nuclear Data Evaluation with the TALYS Code System *Nuclear Data Sheets*, 113, (2012) 841-2934.
4. M. Herman et al EMPIRE: Nuclear Reaction Model Code System for Data Evaluation *Nuclear Data Sheets*, vol. 108, Issue 12 (2007) 2655-2715.
5. Mayank Rajput et al, Calculated differential and double differential cross section of DT neutron induced reactions on natural chromium (Cr) *Indian J Phys*, vol. 92 (2018) 91-96.
6. Mayank Rajput et al Primary knock on atom spectra, gas production and displacement cross section for tungsten and chromium irradiated with neutrons at energies up to 14.1 MeV *Fusion Engineering and Design* 130 (2018) 114–121.
7. Mayank Rajput et al Neutron induced Primary knock on spectra and displacement damage on fusion reactor materials (W, Fe, Cr, Cu& Al) at energies up to 14.1 MeV energy 30th edition of the Symposium on Fusion Technology (2018).
8. M. I. Norgett et al A proposed method of calculating displacement dose rates *Nuclear engineering and design* 33 (1975) 50-54.
9. Kai Nordlund et al, Improving atomic displacement and replacement calculations *Nature communication*, DOI: 10.1038/s41467-018-03415-5.
10. J. Knaster et al Material research for fusion *Nature physics*, 12 (2016) 424-434.
11. M. Warriar et al Statistical study of defects caused by primary knock-on atoms in fcc Cu and bcc W using molecular dynamics *Journal of Nuclear Materials* 467 1 (2015) 457-464.
12. Fikar et al Molecular dynamics simulation of radiation damage in bcc tungsten *Nucl. Instrum. Methods Phys. Res. B* 255 (2007) 27-31
13. R.E. Stoller, Primary radiation damage formation, *Comprehensive Nuclear Materials*, vol.1, 2012, pp. 293-332. Elsevier.
14. R.E. Stoller et al Statistical analysis of a library of molecular dynamics cascade simulations in iron at 100 K *J. Nucl. Mater.* 283 5 (2000) 746-752.
15. S.J. Plimpton Fast Parallel Algorithms for Short-Range Molecular Dynamics *J. Comput. Phys.* 117 (1995) 1-19.
16. A. Stukowski et al, Extracting dislocations and non-dislocation crystal defects from atomistic simulation data *Modelling Simul. Mater. Sci. Eng.* 18 (2010).
17. X.W. Zhou et al Atomic scale structure of sputtered metal multilayers *Acta Mater.* 49 (19) (2001) 4005.
18. Malerba et al. Comparison of empirical interatomic potentials for iron applied to radiation damage studies *Journal of Nuclear Materials*, 406 1 (2010) 19-38.
19. DA Brown et al ENDF/B-VIII.0: The 8th Major Release of the Nuclear Reaction Data Library with CIELO-project Cross Sections, New Standards and Thermal Scattering Data *Nuclear Data Sheets* 148 (2018) 1-142.
20. AJ Konning et al TENDL-2015: TALYS evaluated nuclear data library, https://tendl.web.psi.ch/tendl_2015/tendl2015.html
21. Yu .E. Kozyr et al, Radiative transitions from unbound states of fe and co nuclei *Soviet Journal of Nuclear Physics*, 27, (1978) 329-335.
22. SM Grimes et al Charged particle emission in reactions of 15-MeV neutrons with isotopes of chromium, iron, nickel, and copper *Physical Review C* 19 (1979) 2127-2235.
23. R. Fischer et al Investigation of the fe-56(n,a)cr-53 and ni-60(n,a)fe-57 reactions *Physical Review C* 34 (1986) 460-467.
24. G. J. Ackland et al The MOLDY short-range molecular dynamics package *Computer Physics Communications*, 182 12 (2011) 2587-2604.
25. Gilbert et al, Neutron-induced transmutation effects in W and W-alloys in a fusion environment *Nucl. Fusion* 51 (2011) 13.